Applied Microbiology and Biotechnology (2022) 106:2147–2159
https://doi.org/10.1007/s00253-022-11847-9

APPLIED MICROBIAL AND CELL PHYSIOLOGY

Crossregulation of rapamycin and elaiophylin biosynthesis by RapH in *Streptomyces rapamycinicus*

Wenyan He[1] · Wenfang Wang[1] · Jiaxiang Ma[1] · Guosong Zheng[1] · Andrei A. Zimin[2] · Weihong Jiang[3] · Jinzhong Tian[3] · Yinhua Lu[1,4]

Received: 9 December 2021 / Revised: 16 February 2022 / Accepted: 20 February 2022 / Published online: 26 February 2022

Abstract

Rapamycin is an important macrocyclic antibiotic produced by *Streptomyces rapamycinicus*. In the rapamycin biosynthetic gene cluster (BGC), there are up to five regulatory genes, which have been shown to play important roles in the regulation of rapamycin biosynthesis. Here, we demonstrated that the rapamycin BGC-situated LAL family regulator RapH coordinately regulated the biosynthesis of both rapamycin and elaiophylin. We showed that *rapH* overexpression not only resulted in enhanced rapamycin production but also led to increased synthesis of another type I polyketide antibiotic, elaiophylin. Consistent with this, *rapH* deletion resulted in decreased production of both antibiotics. Through real-time RT-PCR combined with β-glucuronidase reporter assays, four target genes controlled by RapH, including *rapL* (encoding a lysine cyclodeaminase)/*rapH* in the rapamycin BGC and *ela3* (encoding a LuxR family regulator)/*ela9* (encoding a hypothetical protein) in the elaiophylin BGC, were identified. A relatively conserved signature sequence recognized by RapH, which comprises two 4-nt inverted repeats separated by 8-nt, 5′-GTT/AC-N_8-GTAC-3′, was defined. Taken together, our findings demonstrated that RapH was involved in co-ordinated regulation of two disparate BGCs specifying two unrelated antibiotics, rapamycin and elaiophylin. These results further expand our knowledge of the regulation of antibiotic biosynthesis in *S. rapamycinicus*.

Key points

- *The cluster-situated regulator RapH controlled the synthesis of two antibiotics.*
- *Four promoter regions recognized by RapH were identified.*
- *A 16-nt signature DNA sequence essential for RapH regulation was defined.*

Keywords Cluster-situated regulator · Rapamycin · Elaiophylin · *Streptomyces rapamycinicus*

Wenyan He and Wenfang Wang contributed equally to this study.

✉ Jinzhong Tian
tianjinzhong@cemps.ac.cn

✉ Yinhua Lu
yhlu@shnu.edu.cn

[1] College of Life Sciences, Shanghai Normal University, Shanghai 200234, China

[2] G.K. Scriabin Institute of Biochemistry and Physiology of Microorganisms RAS, Pushchino 142290, Russia

[3] Key Laboratory of Synthetic Biology, CAS Center for Excellence in Molecular Plant Sciences, Shanghai Institute of Plant Physiology and Ecology, Chinese Academy of Sciences, Shanghai 200032, China

[4] Development Center of Plant Germplasm Resources, College of Life Sciences, Shanghai Normal University, Shanghai 200234, China

Introduction

Rapamycin is an important macrocyclic polyketide antibiotic produced by several actinomycete strains, including *Streptomyces rapamycinicus* (initially named as *Streptomyces hygroscopicus* ATCC 29,253 or NRRL 5491) (Vezina et al. 1975), *Streptomyces iranensis* (Hamedi et al. 2010; Horn et al. 2014), and *Actinoplanes* sp. N902-109 (Huang et al. 2015a). This compound shows antifungal (Vezina et al. 1975), immunosuppressive (Martel et al. 1977), and anticancer activities (Houchens et al. 1983) as well as neuroprotective/neuroregenerative properties (Malagelada et al. 2010; Pan et al. 2008; Tain et al. 2009; Yoo et al. 2017). Rapamycin is mainly licensed for use as an immunosuppressant for the treatment of patients receiving solid organ transplants.

In addition, rapamycin derivatives have been approved as anticancer agents in the treatment of renal cell carcinoma and lymphoid malignancies (Argyriou et al. 2012; Zhou and Huang 2012). The immense pharmacological importance of rapamycin and its derivatives has led to a great demand for its economic production at an industrial scale.

In recent decades, much progress has been made in understanding of the rapamycin biosynthetic pathway and the mechanisms regulating this pathway (Park et al. 2010; Schwecke et al. 1995; Yoo et al. 2017); these findings have facilitated strain improvement for rapamycin overproduction by metabolic engineering approaches (Park et al. 2010; Yoo et al. 2017). Rapamycin is produced by a hybrid type I polyketide synthase (PKS)/non-ribosomal peptide synthetase (NRPS) system. The rapamycin polyketide backbone is synthesized by three multifunctional modular PKSs, including RapA, RapB, and RapC, using (4*R*,5*R*)-4,5-dihydrocyclohex-1-ene-carboxylic acid (DHCHC) as a starter unit (Andexer et al. 2011; Aparicio et al. 1996; Gregory et al. 2004) and 14 molecules of (2*S*)-malonyl-CoA and (2*S*)-methylmalonyl-CoA as extension units (Paiva et al. 1991). The linear polyketide chain is condensed with the lysine-derived pipecolate via the NRPS RapP, and then cyclized to produce pre-rapamycin (Konig et al. 1997; Schwecke et al. 1995). The final product, rapamycin, is finally synthesized after modification of pre-rapamycin by a series of post-PKS tailoring steps (e.g., O-methylation and hydroxylation) (Chung et al. 2001; Park et al. 2010; Yoo et al. 2017). The rapamycin biosynthetic gene cluster (BGC), which covers a total of 107 kb and contains 26 open reading frames (ORFs), has been cloned (Schwecke et al. 1995). Interestingly, there are up to five regulatory genes located in the rapamycin BGC, namely, *rapR/S*, *rapY*, *rapG*, and *rapH*, suggesting that the regulatory network mediating rapamycin biosynthesis is complex. The functions of these five regulators have been preliminarily identified. Among them, *rapS/R*, which encodes a histidine kinase (HK) and a response regulator (RR), forming a typical two-component system, and *rapY*, which encodes a TetR-family regulator, have been identified as repressors of rapamycin biosynthesis (Yoo et al. 2015). *rapG* and *rapH*, which encode an AraC family regulator and an LAL (the large ATP-binding regulators of the LuxR) family regulator, respectively, have been shown to function as activators of rapamycin biosynthesis (Kuscer et al. 2007).

In this study, we showed that overexpression or deletion of the cluster-situated regulatory gene *rapH* not only resulted in significantly altered rapamycin production but also obviously affected the production of another type I polyketide antibiotic, elaiophylin. This compound is a 16-membered macrodiolide with C2 symmetry, which has various biological activities, including antibacterial (Wu et al. 2013), antihelmintic (Hammann et al. 1990), antitumor (Zhao et al. 2015), and immunosuppressive activities (Gui et al. 2019). The BGC responsible for elaiophylin biosynthesis is located nearly 8.28 Mb away from the rapamycin BGC on the genome of *S. rapamycinicus*. We also investigated the mechanism underlying RapH-mediated crossregulation of rapamycin and elaiophylin biosynthesis. Our findings further expand our knowledge of the regulation of secondary metabolism in *S. rapamycinicus*.

Materials and methods

Strains, plasmids, primers, and bacterial growth conditions

All strains and plasmids used in this study are presented in Table S1 and primers are listed in Table S2 in the supplemental materials. *S. rapamycinicus* NRRL 5491 and derivatives were cultured on oat agar medium (20 g/L oat, 20 g/L agar, pH 6.8) at 30 °C for spore preparation and on M-ISP$_4$ (5 g/L starch, 1 g/L yeast extract, 2 g/L tryptone, 5 g/L soya flour, 5 g/L mannitol, 1 g/L sodium chloride, 2 g/L calcium carbonate, 2 g/L ammonium sulfate, 0.5 g/L valine, 20 g/L agar) for intergenic conjugation. Seed medium (20 g/L soluble starch, 1 g/L L-lysine, 1.2 g/L $K_2HPO_4{\cdot}3H_2O$, 10 g/L peptone, 6 g/L yeast extract, 10 g/L glucose, pH 6.65) and fermentation medium (10 g/L soybean flour, 20 g/L corn dextrin, 6 g/L yeast extract, 2 g/L peptone, 40 g/L oat, 5 g/L NaCl, 10 g/L glycerol, 2.5 g/L L-lysine, 40 g/L glucose, pH 6.42), were used for *S. rapamycinicus* fermentation. *S. coelicolor* M1146 (M145Δ*act*Δ*red*Δ*cda*Δ*cpk*) (Gomez-Escribano and Bibb. 2011) and derivatives were cultured at 30 °C on MS agar medium (20 g/L soya flour, 20 g/L mannitol, 20 g/L agar) for spore suspension preparation as well as intergenic conjugation, and AS-1 medium (1 g/L yeast extract, 0.2 g/L L-lysine, 0.2 g/L L-arginine, 0.2 g/L L-asparagine, 5 g/L soluble starch, 2.5 g/L NaCl, 10 g/L Na_2SO_4, 20 g/L agar) was used for GUS assays. *Escherichia coli* Top10 was used as the host for general DNA cloning. *E. coli* ET12567/pUZ8002 (a methylation-deficient strain) or S17-1 (a methylation-rich strain) was employed as the donor strain in conjugal transfer between *E. coli* and *S. rapamycinicus* or *S. coelicolor* (Kieser et al. 2000). *E. coli* was grown at 37 °C in Luria–Bertani (LB) broth with shaking at 200 rpm or on LB agar. Antibiotics were selectively added into the medium at the following concentrations: apramycin (50 μg/mL), kanamycin (50 μg/mL), chloramphenicol (50 μg/mL), and nalidixic acid (25 μg/mL).

Construction of the Δ*rapH* mutant

The Δ*rapH* mutant with an in-frame deletion of partial *rapH* ORF (encoding the RapH protein fragment from 499 to 873 aa) was constructed by the CRISPR/Cas9 genome

editing technology (Huang et al. 2015b). Briefly, a DNA fragment specifying the synthesis of a specific single guide RNA (sgRNA^{rapH}) targeting *rapH* was amplified from the template pKCCas9dO using the primer pair sgRNA-fw/rev. The upstream and downstream homology arms (approximately 1.1 kb each) flanking the *rapH* DNA fragment to be deleted were amplified from *S. rapamycinicus* NRRL 5491 using the primer pairs of rapH-up-fw/rev and rapH-down-fw/rev, respectively. The above three products were ligated together by overlapping PCR to generate sgRNA^{rapH}-UD. After digestion with *Spe*I/*Hin*dIII, sgRNA^{rapH}-UD was cloned into pKCCas9dO treated with the same two restriction enzymes, resulting in the recombinant editing plasmid pKCCas9-sgRNA^{rapH}-UD. The obtained plasmid was introduced into *S. rapamycinicus* via intergenic conjugation. The positive exoconjugants were verified by colony PCR using the primer pair rapH(qs)-fw/rev and DNA sequencing. The edited strain was passaged at 37 °C on oat agar without antibiotics for three times to remove pKCCas9-sgRNA^{rapH}-UD, generating the Δ*rapH* mutant.

Construction of the complemented strain Δ*rapH*/pIB-*rapH* and the *rapH* overexpression strain WT/pIB-*rapH*

Based on the integrative vector pIB139 (Wilkinson et al. 2002), the recombinant plasmid pIB-*rapH* with *rapH* overexpression under the control of the constitutive promoter *ermEp** was constructed as follows. The *rapH* gene was amplified from *S. rapamycinicus* genomic DNA using the primer pair rapH-fw/rev. The PCR product was digested with *Nde*I/*Xba*I and then cloned into pIB139 treated with the same two restriction enzymes, generating pIB-*rapH*. The correctness of the recombinant plasmid was verified by DNA sequencing. The obtained plasmid was introduced into the wild-type strain (WT) and the Δ*rapH* mutant by conjugal transfer, respectively, resulting in the *rapH* overexpression strain WT/pIB-*rapH* and the complemented strain Δ*rapH*/pIB-*rapH*. As controls, two strains, WT/pIB139 and Δ*rapH*/pIB139, were constructed by introducing the empty plasmid pIB139 into the wild-type strain and the Δ*rapH* mutant, respectively.

Analysis of rapamycin and elaiophylin production

S. rapamycinicus strains were cultured on oat agar plates for 12 days. Agar cultures (approximately 1 cm^2) were inoculated into 25 mL of seed medium and grown for 24 h at 28 °C on a rotary shaker (240 rpm). Then, 3 mL of seed cultures was transferred into 30 mL of fermentation medium in 250-mL flasks. Of fermentation samples, 0.5 mL was collected at four time points (5, 7, 9, and 11 days) and extracted with equal volume of ethanol at room temperature for 1 h. After centrifugation at 12, 000 rpm for 10 min, supernatants were analyzed by high-performance liquid chromatography (HPLC) using a reversed-phase column (Hypersil ODS2, 5 um, 4.6 × 250 mm). The mobile phase was a mixture of methanol and water (85%:15%) with a flow rate of 1.0 mL/min. Rapamycin and elaiophylin were detected at a wavelength of 277.4 nm. *S. rapamycinicus* fermentation was performed with three independent biological replicates, each having three technical replicates. Error bars represent the standard deviations (SD) of three independent experiments. Statistical analysis was conducted by a two-tailed Student's *t* test.

High-resolution tandem mass spectrometry (HR-MS/MS) analysis of elaiophylin was performed on the 6230B Accurate Mass TOF LC/MS System (Agilent Technologies Inc., USA). To obtain the electrospray mass spectra of all peaks, the TIC-negative mode was used and the MS parameters are as follows: mass range 200–1300 m/z (with MS scan rate 1.03 and resolution ± 0.5 amu), nebulizer 40 psi, gas (N_2) temperature 350 °C, gas flow 9 L/min, VCap 3500 V, Fragmentor 160 V, Skimmer 65 V, Octopole RF 750 V, and Ext Dyn standard 2 GHz (3200). The temperature of the ion spray was maintained at 21 ± 1 °C. To further validate the elaiophylin peaks, the MS/MS-negative ion mode mass spectrometry was employed. The MS/MS parameters are the same as those described in TIC above, except MS/MS range 50–1100 m/z and collision energy 35 V.

Construction of the *gusA* reporter systems for GUS assays

The *gusA* reporter system was used to determine the direct target genes of RapH as described previously (Guan et al. 2019; Myronovskyi et al. 2011; Zhang et al. 2016). Totally, three possible promoter regions in the rapamycin BGC (*rapHp*, *rapLp*, and *rapKp*) and five putative promoter regions in the elaiophylin BGC (*elaMp*, *ela3p*, *ela5p*, *ela6p*, and *ela9p*) were tested to drive the expression of the *gusA* gene (encoding a β-glucuronidase) (Table S3). Here, we gave a brief introduction of the construction process of the *gusA* reporter systems using *rapLp*-driven *gusA* reporter as an example. The *rapLp* promoter region was amplified from *S. rapamycinicus* NRRL 5491 by PCR with primer pair rapLp-fw/rev. The *gusA* gene was amplified from pSET-*hrdBp-gusA* (Zhang et al. 2016) by PCR using the primer pair gusA-fw/rev. The PCR products of *rapLp* and *gusA* were ligated together by overlapping PCR using the primer pair rapLp-fw/gusA-rev to yield *rapLp-gusA* fragment. After digestion with *Xba*I/*Eco*RI, it was cloned into pSET152 treated with the same two enzymes, resulting in the reporter plasmid pSET-*rapLp-gusA*. Other seven reporter plasmids (Table S1) were constructed similarly.

These reporter plasmids were individually integrated into the ΦC31 *attB* site of *S. coelicolor* M1146 by intergenic conjugation. Exoconjugants were streaked on MS agar with apramycin to obtain the recombinant strains (e.g., M1146/pSET-*rapLp-gusA*) (Table S1).

To achieve *rapH* overexpression in the above engineered strains containing tested promoter-driven *gusA* reporter gene, the recombinant plasmid pRT-*rapH* was constructed based on the integrative plasmid pRT802 with the ΦBT1 *attB* site and kanamycin-resistant marker. Briefly, the *rapH* coding region was amplified from *S. rapamycinicus* NRRL 5491 using the primer pair rapH-fw/rev. The *ermEp** promoter used to drive *rapH* expression was obtained by PCR from pIB139 using the primer pair ermEp*-fw/rev. Two PCR products were ligated together by overlapping PCR using the primers ermEp*-F/rapH-rev to yield *ermEp*-rapH*, which was cloned into pRT802 between the enzyme sites of *Spe*I/*Eco*RI to generate pRT-*rapH*. The obtained plasmid was introduced into *S. coelicolor* M1146 derivatives containing tested promoter-driven *gusA* reporter systems (e.g., M1146/pSET-*rapLp-gusA*) via ΦBT1-integrase-based integration by intergenic conjugation between *S. coelicolor* and S17-1. Exoconjugants were selected on MS agar with kanamycin, resulting in the recombinant strains (e.g., M1146/pSET-*rapLp-gusA*/pRT-*rapH*) harboring both the *rapH* overexpression plasmid (pRT-*rapH*) and the *gusA* reporter plasmid (e.g., pSET-*rapL-gusA*).

For GUS assays, 5-μL spores of *S. coelicolor* strains with the same concentration (OD450 = 1.0) were spotted on AS-1 agar plates (25-mL) containing 50 μL of 25 mg/mL 5-bromo-4-chloro-3-indolyl-β-D-glucuronide (X-Gluc). Changes in blue color were compared between M1146 derivatives only containing tested promoter-driven *gusA* reporter (e.g., M1146/pSET-*rapLp-gusA*) and the corresponding recombinant strains, namely, M1146 containing both pRT-*rapH* and the *gusA* reporter plasmid (e.g., M1146/pSET-*rapLp-gusA*/pRT-*rapH*/). The plates were photographed after bacterial growth at 30 °C for 3 days.

RNA isolation and real-time reverse transcription-PCR (RT-qPCR)

Fermentation cultures (20 mL) of the *S. rapamycinicus* strains were collected at two time points (at 5 and 9 days) by centrifugation (8000 rpm, 10 min). Precipitated bacterial cells were taken, and immediately frozen and ground into powder in liquid nitrogen. RNA samples were extracted using the Ultrapure RNA Kit (SparkJade, Shanghai, China) according to the procedure recommended by the manufacturer. RNA preparations were digested with DNase I (SparkJade, Shanghai, China) (2 U DNase I/1 μg RNA) to remove the residual genomic DNA. The quality and quantity of RNA samples were analyzed via agarose gel electrophoresis and UV spectroscopy.

Synthesis of cDNA was carried out using approximately 1 μg RNA with the Novizan's HiScript® II 1st Strand cDNA Synthesis Kit according to the manufacturer's instructions. RT-qPCR was carried out in a MyiQ2™ two-color real-time PCR Analyzer (Bio-Rad, USA), using ChamQ Universal SYBR Green qPCR Master Mix kit. PCR reactions were performed in triplicate for each gene and repeated with two biological replicates. The *hrdB* gene (*M271_14880*, encoding the principal sigma factor), whose expression was verified to be constant in both the wild-type and the Δ*rapH* mutant under the tested experimental conditions (Fig. S1), was selected as an internal control. The relative transcript levels of each gene were normalized to those of *hrdB*. Relative fold changes in the transcript levels of tested genes (Δ*rapH*/WT) were measured using the $2^{-\Delta\Delta Ct}$ method (Livak and Schmittgen. 2001). Error bars represent the standard deviations (SD) from two independent experiments using two biological replicates. Statistical analysis was conducted by a two-tailed Student's *t* test.

Site-directed mutagenesis

Site-directed mutagenesis of the signature sequence recognized by RapH in the promoter regions of *rapL* and *ela3* in the plasmids of pSET-*rapLp-gusA* and pSET-*ela3p-gusA* was carried out using two rounds of PCR amplification according to the method described previously (Liu and Naismith. 2008). Briefly, in the first round, PCR was conducted with forward primer (rapLpmut-fw or ela3pmut-fw) and reverse primer (rapLpmut-rev or ela3pmut-rev), respectively, and the plasmid (pSET-*rapLp-gusA* or pSET-*ela3p-gusA*) was used as the template. PCR was carried out in 20 μL volume, which contains 100 ng of template DNA, 10 μM primers, 5 mM dNTPs, and 1 unit of high-fidelity DNA polymerase. PCR reactions were initiated at 98 °C for 1 min, followed by 12 amplification cycles. Each cycle consists of 98 °C, 10 s; 58 °C, 20 s; and 68 °C, 5 min. In the second round, two PCR products from the first PCR round were mixed and 1 unit of high-fidelity PCR polymerase was added, followed by 16 amplification cycles. The PCR parameters are the same as the first round. Forty microliters of the final PCR products was treated with 2 U of the restriction enzyme *Dpn*I to remove the methylated template plasmid at 37 °C for 2 h. Five microliters of the above PCR products was transformed into *E. coli* Top10 competent cells. Transformants were cultured in LB liquid medium and the plasmids were extracted using the Tolobio Plasmid Extraction Kit (Tolobio, Shanghai, China) and mutant plasmids with correct targeted mutations were verified by DNA sequencing. The obtained plasmids were transferred into *S. coelicolor* M1146 by intergenic conjugation to generate M1146/

pSET-*rapLpmu-gusA* and M1146/pSET-*ela3pmu-gusA*. Then, pRT-*rapH* was integrated into the above two mutant strains, resulting in M1146/pSET-*rapLpmu-gusA*/pRT-*rapH* and M1146/pSET-*ela3pmu-gusA*/pRT-*rapH*. GUS assays were conducted as described above. Four strains, M1146/pSET-*rapLp-gusA*, M1146/pSET-*rapLp-gusA*/pRT-*rapH*, M1146/pSET-*ela3-gusA*, and M1146/pSET-*ela3-gusA*/pRT-*rapH*, were used as controls.

Determination of transcription start sites (TSSs)

5′-rapid amplification of cDNA ends (5′-RACE) was carried out to determine the transcriptional start sites (TSSs) of *rapL* and *ela3* using 5′-RACE kit (Sangon, Shanghai, China) according to the manufacturer's instructions. Two rounds of PCR amplification (including a nested PCR) were conducted with the primers listed in Table S2. The amplified 5′-RACE products were cloned into the pMD-18 T simple vector (TaKaRa, Japan). The cloned sequences from ten recombinant plasmids were determined by DNA sequencing. If over seven of the sequenced cDNA ends were identical, the 5′-end was considered the TSS.

Results

Involvement of *rapH* in the positive regulation of rapamycin and elaiophylin biosynthesis

In an attempt to improve rapamycin production by *rapH* overexpression, we found that introduction of the *rapH* overexpression plasmid pIB-*rapH* into the wild-type (WT) strain of *S. rapamycinicus* resulted in increased rapamycin production; however, interestingly, the synthesis of an unrelated product was also significantly upregulated in the engineered strain WT/pIB-*rapH*, according to HPLC analysis of fermentation samples (Fig. 1A).

To identify the chemical structure of this product, we first detected the ultraviolet absorption spectrum of the compound and found that its characteristic absorption peak was at 252 nm (Fig. 1B), consistent with that of the known compound, elaiophylin, produced by *S. rapamycinicus* (Fang et al. 2000). Subsequently, the product was analyzed and compared with the elaiophylin standard

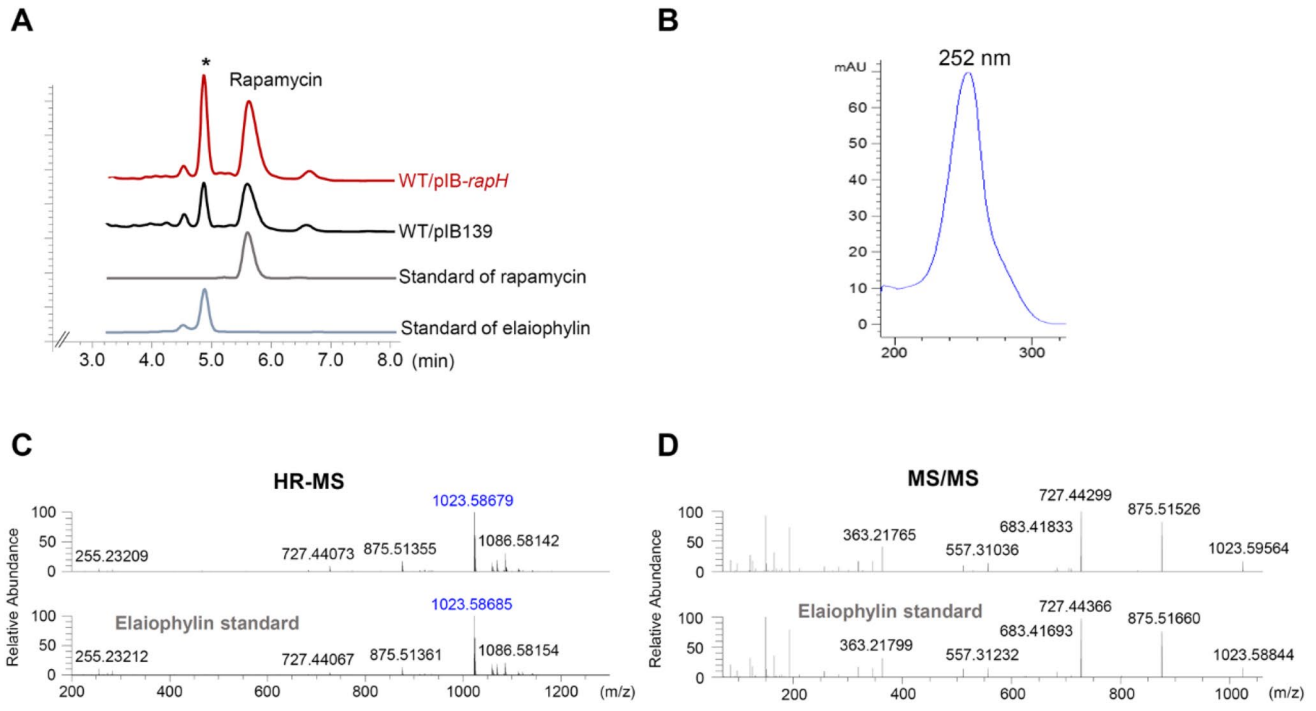

Fig. 1 Analysis of the unrelated product (elaiophylin) with improved production levels in the *rapH* overexpression strain WT/pIB-*rapH*. **A** HPLC analysis of the fermentation culture of the *rapH* overexpression strain WT/pIB-*rapH*. The fermentation culture of WT/pIB139 was used as a control. HPLC profiles of the standards of elaiophylin and rapamycin were also presented. **B** Absorption wavelength of the unrelated product (elaiophylin) overproduced in WT/pIB-*rapH*. **C** HR-MS analysis of the unrelated product (elaiophylin) overproduced in WT/pIB-*rapH*. The standard of elaiophylin was used as a control. **D** MS–MS analysis of the unrelated product (elaiophylin) overproduced in WT/pIB-*rapH*. The standard of elaiophylin was used as a control

using high-resolution tandem mass spectrometry (HR-MS/MS). We found that the MS spectra were consistent with those of the elaiophylin standard. HR-MS analysis revealed that this unrelated product exhibited a molecular ion at m/z = 1023.586 ([M-H]-), similar to the elaiophylin standard (Fig. 1C). Further MS/MS analysis showed that the fragment ions produced also matched well with the standard (Fig. 1D). Therefore, this compound was identified as elaiophylin. The BGCs responsible for elaiophylin biosynthesis have been identified in other *Streptomyces* strains, including *Streptomyces* sp. M56 and *Streptomyces malaysiensis* DSM4137 (Haydock et al. 2004; Klassen et al. 2019). Using the online software antiSMASH (https://antismash.secondarymetabolites.org/), we identified the elaiophylin BGC in *S. rapamycinicus* NRRL 5491, which exhibited a genetic organization similar to that of the reported elaiophylin BGC (Fig. S2) and was located nearly 8.28 Mb away from the rapamycin BGC.

Next, the effects of *rapH* overexpression on rapamycin and elaiophylin production were quantitatively determined. Two strains, WT/pIB139 and WT/pIB-*rapH*, were grown in fermentation medium and cultures were collected at four time points (5, 7, 9, and 11 days) for HPLC analysis of antibiotic production. We showed that the engineered strain WT/pIB-*rapH* produced rapamycin and elaiophylin titers that were 39.8–46.5% and 9.3–20.4% higher than those of the control strain WT/pIB139 (Fig. 2A, B).

To further confirm the roles of RapH in the regulation of rapamycin and elaiophylin biosynthesis, a Δ*rapH* mutant with a partial in-frame deletion of *rapH* was constructed (Fig. S3), and its phenotypic changes were compared with those of the WT strain. We observed that deletion of *rapH* had no visible effect on cell growth or morphological differentiation on oat agar medium (data not shown). Further investigation of the effects of *rapH* deletion on rapamycin and elaiophylin production using HPLC analysis revealed that deletion of *rapH* resulted in reduced production of both antibiotics. Rapamycin titers of the Δ*rapH* mutant were decreased to a very low level throughout the tested time course, as reported previously (Kuscer et al. 2007), and elaiophylin production was reduced by at most 29.3% compared with that in the WT strain (Fig. 2C, D). To verify that the phenotypic changes in the mutant were caused by *rapH* deletion, the plasmid pIB-*rapH* was introduced into the mutant to yield Δ*rapH*/pIB-*rapH*. As controls, the empty plasmid pIB139 was introduced into the WT strain and the Δ*rapH* mutant, generating WT/pIB139 and Δ*rapH*/pIB139. HPLC analysis of fermentation cultures showed that the

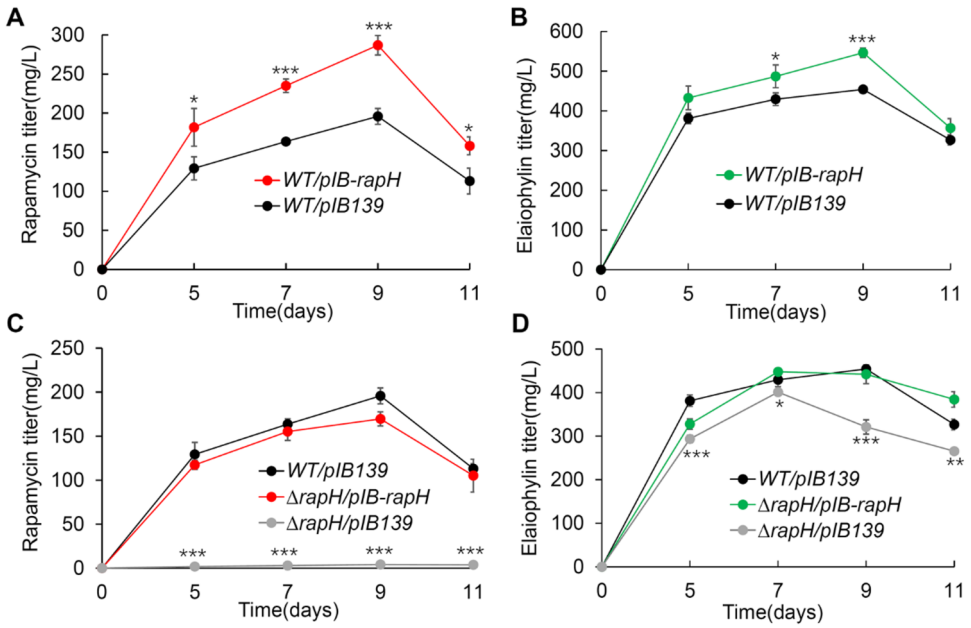

Fig. 2 Effects of *rapH* overexpression or deletion on rapamycin and elaiophylin biosynthesis. Introduction of the *rapH* overexpression plasmid pIB-*rapH* into the wild-type (WT) strain led to enhanced production of both rapamycin (**A**) and elaiophylin (**B**). Deletion of *rapH* resulted in markedly reduced rapamycin production (**C**) and obviously decreased elaiophylin biosynthesis (**D**). The reduced rapamycin and elaiophylin production in the Δ*rapH* mutant could be complemented by introduction of pIB-*rapH*. Samples were collected from *S. rapamycinicus* strains, including WT/pIB-*rapH* (the WT strain with pIB-*rapH*), WT/pIB139 (the WT strain with the empty vector pIB139), Δ*rapH*/pIB139 (the Δ*rapH* mutant with pIB139), and the complemented strain Δ*rapH*/pIB-*rapH* (the Δ*rapH* mutant with pIB-*rapH*), grown in fermentation medium at four time points (5, 7, 9, and 11 days), respectively. Error bars denote standard deviations (SD) of three biological replicates, each having three technical replicates. Statistical analysis was conducted using a two-tailed Student's *t* test. ***, $P < 0.001$; **, $P < 0.01$; *, $P < 0.05$ vs. the control strain (WT/pIB139)

titers of rapamycin and elaiophylin of the complemented strain (Δ*rapH*/pIB-*rapH*) could be restored to the levels of WT/pIB139, whereas the mutant strain with pIB139 (Δ*rapH*/pIB139) produced lower levels of both antibiotics compared with WT/pIB139 (Fig. 2C, D). The above data confirmed that RapH functioned as an activator for the biosynthesis of both rapamycin and elaiophylin, which provides novel insights into of the roles of RapH in *S. rapamycinicus*.

Transcriptional analysis of the rapamycin and elaiophylin BGCs upon *rapH* deletion

To assess the function of RapH on rapamycin and elaiophylin biosynthesis at the transcription level, the effects of *rapH* deletion on the transcription of these two antibiotic BGCs were checked by RT-qPCR analysis. Because many genes in these two BGCs transcribed in the same direction either overlapped or were separated by short intergenic regions (Figs. 3A and 4A), we first performed co-transcriptional analysis to determine the genetic organization of these two BGCs. Notably, the genes transcribed in the same direction, such as *rapRS*, *rapAB*, *rapNO*, and *rapJI*, in the rapamycin BGC, overlapped by 4 bp or more than 4 bp, implying that these genes were likely to be co-transcribed. Therefore, these genes were not subjected to co-transcriptional analysis. In addition, the reverse PCR primers were designed to target the sequences over 250 bp away from the start codons (ATG or GTG) of the downstream genes to minimize the possibility that the co-transcribed products were generated as readthrough transcripts. The results revealed the presence of totally 13 transcriptional units in both the rapamycin and elaiophylin BGC (Figs. 3B and 4B).

Next, RT-qPCR was performed to compare the transcript levels of these different transcriptional units between the WT strain and the Δ*rapH* mutant. For each transcription unit, one gene was selected for transcriptional analysis. Total RNA samples were extracted from the fermentation cultures of these two strains after growth for 5 and 9 days. RT-qPCR analysis showed that, in the rapamycin BGC, *rapH* and *rapL* were downregulated by approximately five-fold and three-fold, respectively, whereas *rapK* was upregulated by approximately three-fold, upon *rapH* deletion (Fig. 3C). According to the results of co-transcriptional analysis, we know that *rapL* and *rapK* are co-transcribed with *rapMNO* and *rapJI*, respectively, suggesting that these two operons, *rapLMNO* and *rapKJI*, were regulated by RapH. This was

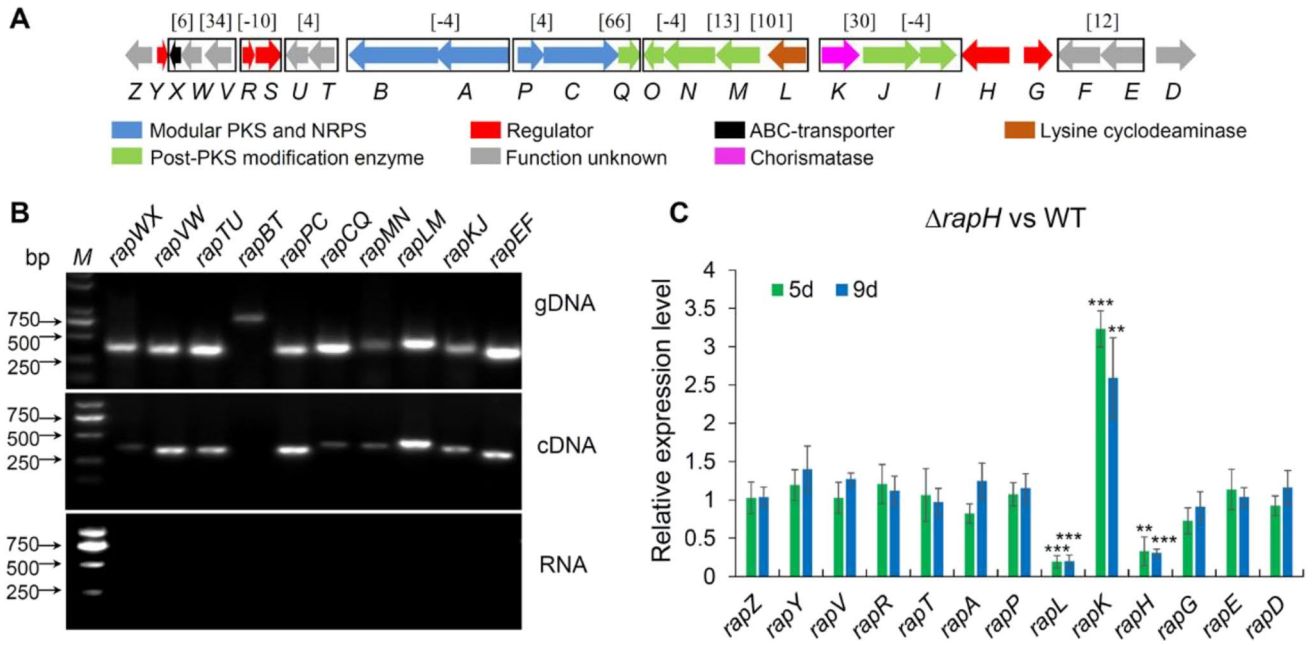

Fig. 3 Transcriptional analysis of the rapamycin BGC upon *rapH* deletion. **A** Genetic organization of the rapamycin BGC in *S. rapamycinicus*. Co-transcribed genes are indicated by black boxes. The numbers in square brackets indicate the lengths of DNA sequence between two adjacent genes transcribed in the same direction. **B** Co-transcriptional analysis of the rapamycin BGC by RT-PCR. RNA samples were isolated from the WT strain grown in fermentation medium for 5 days. Genomic DNA (gDNA) and RNA without reverse transcription were used in PCR reactions as the positive and negative controls, respectively. **C** Transcriptional analysis of the rapamycin biosynthetic genes upon *rapH* deletion by RT-qPCR. Totally, 13 genes from different operons were selected as indicated. RNA samples were isolated from the fermentation cultures of the WT strain and the Δ*rapH* mutant after growth for 5 and 9 days, respectively. The values were determined after normalization to the internal control, *M271_14880* (*hrdB*, encoding the principal sigma factor). Error bars show the standard deviations (SD) from two independent experiments. Statistical analysis was conducted using a two-tailed Student's *t* test. ***, $P < 0.001$; **, $P < 0.01$ vs. the WT strain

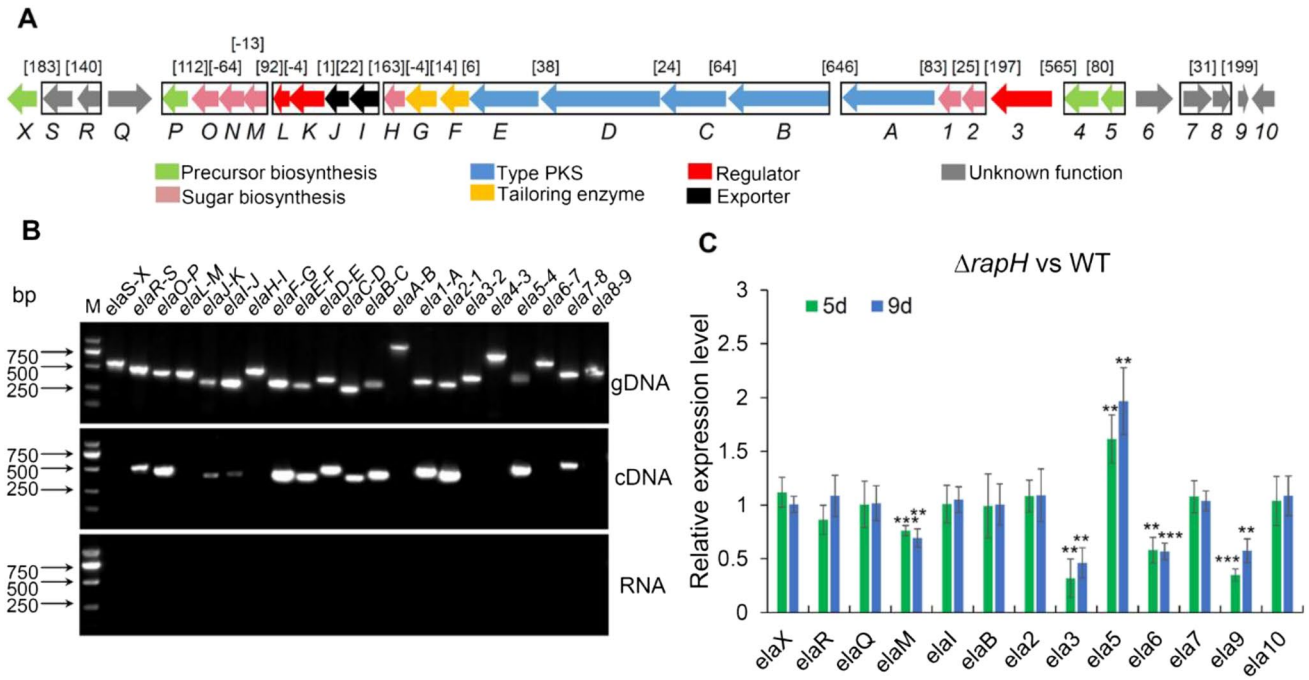

Fig. 4 Transcriptional analysis of the elaiophylin BGC upon *rapH* deletion. **A** Genetic organization of the elaiophylin BGC in *S. rapamycinicus*. Co-transcribed genes are indicated by black boxes. The numbers in square brackets indicate the lengths of DNA sequence between two adjacent genes transcribed in the same direction. **B** Co-transcriptional analysis of the elaiophylin BGC by RT-PCR. RNA samples were isolated from the WT strain grown in fermentation medium for 5 days. Genomic DNA (gDNA) and RNA without reverse transcription were used in PCR reactions as the positive and negative controls, respectively. **C** Transcriptional analysis of the elaiophylin biosynthetic genes upon *rapH* deletion by RT-qPCR. Totally, 13 genes from different operons were selected as indicated. RNA samples were isolated from cultures of the WT strain and the Δ*rapH* mutant grown in fermentation medium for 5 and 9 days, respectively. The values were determined after normalization to the internal control, *M271_14880* (*hrdB*, encoding the principal sigma factor). Error bars show the standard deviations (SD) from two independent experiments. Statistical analysis was conducted using a two-tailed Student's *t* test. ***, $P<0.001$; **, $P<0.01$ vs. the wild-type strain (WT)

further confirmed by RT-qPCR analysis of the expression of *rapMNO* and *rapJI* in the Δ*rapH* mutant (Fig. S4). In the elaiophylin BGC, two genes (*ela3* and *ela9*) were downregulated by up to five- and three-fold whereas *ela5* was upregulated by approximately two-fold upon *rapH* deletion. In addition, we showed that two other genes, i.e., *elaM* and *ela6*, were slightly downregulated in the mutant (Fig. 4C). The *elaM* gene is co-transcribed with *elaNOP*, suggesting that transcription of the whole operon *elaMNOP* was slightly affected by *rapH* deletion; this was further confirmed by RT-qPCR analysis of the expression of *elaNOP* upon *rapH* deletion (Fig. S4). Other genes in these two antibiotic BGCs in the Δ*rapH* mutant were not significantly affected at the transcriptional level compared with that in the WT strain.

RapH directly regulated the promoters of *rapH*, *rapLMNO*, *ela3*, and *ela9*

To determine whether RapH directly regulated the identified target genes or operons, electrophoretic mobility shift assays (EMSAs) were performed firstly. After failure to overexpress the full-length RapH protein, we successfully overexpressed and obtained the purified truncated RapH protein harboring the DNA-binding domain (named His_6-RapHΔ) in *E. coli* BL21 (DE3) (Fig. S5A). However, His_6-RapHΔ did not bind to the tested DNA probes (Fig. S5B), which may be related to loss of the ATP-binding domain in the truncated RapH used in this study.

In a previous study, the *gusA* reporter system, encoding β-glucuronidase (GUS), was successfully employed for the identification of direct target genes regulated by the LAL family regulators MilR and StaR in *Streptomyces bingchenggensis* and *Streptomyces fradiae* CGMCC 4.576, respectively (Guan et al. 2019; Zhang et al. 2016). Therefore, we next used GUS assays to identify the direct target genes of RapH. Eight DNA probes containing the respective promoter regions of *rapLMNO*, *rapKJI*, *rapH*, *elaMNOP*, *ela3*, *ela54*, *ela6*, and *ela9* were cloned separately upstream of *gusA* in pSET152. Eight resulting plasmids were individually integrated into the ΦC31 *attB* site of *S. coelicolor* M1146, generating eight recombinant strains as negative controls (Table S1). The *rapH* gene was cloned downstream of *ermEp** in the integrative plasmid pRT802 to generate pRT-*rapH*. Subsequently, pRT-*rapH* was

integrated into the ΦBT1 *attB* sites of eight *S. coelicolor* negative control strains to yield eight tested recombinant strains (Fig. S6). The spores of 16 obtained strains, namely, eight negative control strains and eight tested recombinant strains, were collected. They were quantitatively inoculated on AS-1 plates medium containing the chromogenic substrate X-Gluc, and photographed after growth for 3 days. GUS assays showed that compared with negative control strains, which displayed no color or a slightly blue color, four tested strains containing pSET-*rapHp-gusA*/pRT-*rapH*, pSET-*rapLp-gusA*/pRT-*rapH*, pSET-*ela3p-gusA*/pRT-*rapH*, and pSET-*ela9p-gusA*/pRT-*rapH* exhibited a higher intensity of blue color (Fig. 5A). However, no color change was detected in other four tested recombinant strains compared with the corresponding negative control strains. The results suggested that RapH could recognize the promoter regions of *rapH*, *rapL*, *ela3*, and *ela9*; therefore, the effects of RapH on the four target genes or operons were likely to be direct.

Defining the putative RapH-binding sequence

To identify the specific DNA-binding sequence recognized by RapH, the putative promoter regions upstream of *rapL* (the intergenic region of *rapL/K*), *rapH*, *ela3*, and *ela9* were compared using MEME analysis (https://meme-suite.org/meme/), which revealed the presence of a relatively conserved 16-nt DNA consensus sequence comprising two 4-nt inverted repeats separated by 8-nt, 5′-GTT/AC-N_8-GTAC-3′ (Fig. 5B), in the promoter regions of *rapL* and *ela3*. However, no such signature sequence could be identified upstream of the other two RapH target genes, *rapH* and *ela9*, suggesting the diversity of the DNA sequences recognized by RapH.

To identify nucleotides essential for RapH recognition, the two 4-nt inverted repeats (5′-GTT/AC-N_8-GTAC-3′) in the promoter regions of these two genes, which were likely essential for RapH-mediated regulation, were mutated to 5′-GGGG-N_8-GGGG-3′. The mutated promoter regions were used to drive *gusA* expression (Fig. 5C), yielding two mutated reporter plasmids, namely, pSET-*rapLp*mut-*gusA* and pSET-*ela3p*mut-*gusA*, and the impact of DNA mutations on GUS activity was determined. The two plasmids were introduced into *S. coelicolor* M1146 and M1146/pRT-*rapH*, respectively, to generate the corresponding reporter strains. Finally, GUS assays showed that mutation of the putative RapH-binding motif in the promoter regions of *rapL* and *ela3* resulted in the loss of the production of blue color by the strains with the integration of both mutated promoter-driven *gusA* reporter gene and pRT-*rapH* (Fig. 5D). These results suggested that the 16-nt palindrome sequence may be essential for RapH-mediated regulation of these two target genes.

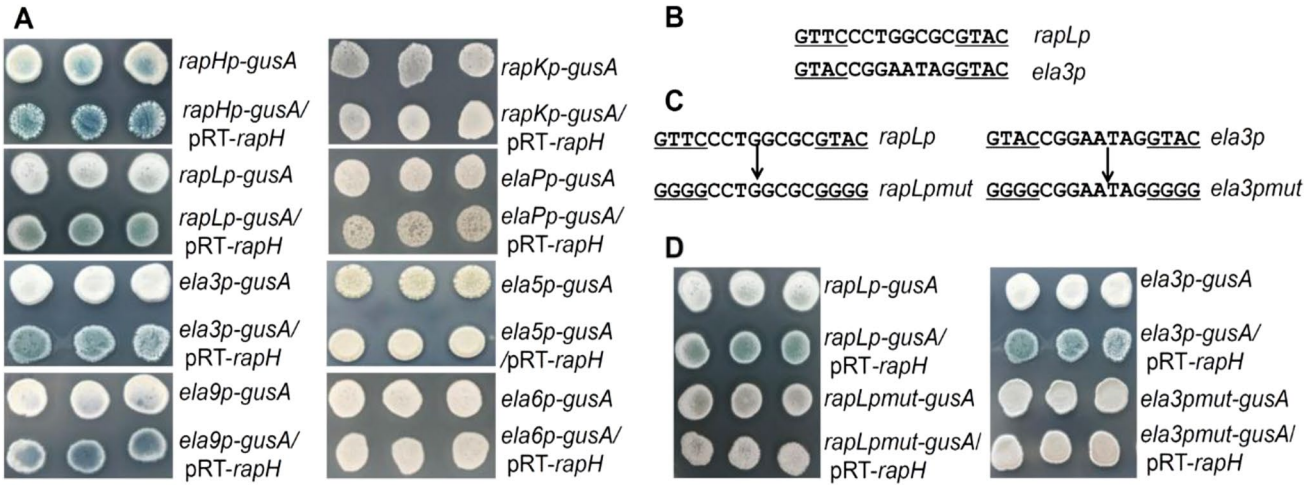

Fig. 5 Identification of target genes directly regulated by RapH and defining the RapH-binding sequences. **A** Chromogenic assays of *S. coelicolor* M1146 derivatives containing the tested promoter-driven *gusA* reporter and/or pRT-*rapH* on AS-1 agar plates. The strains containing both the *gusA* reporter systems and the *rapH* overexpression plasmid (pRT-*rapH*) were cultured at the bottom of each panel. As controls, the strains only containing the *gusA* reporter systems were also shown. The photos were taken after bacterial growth for 3 days. **B** Two 16-nt signature sequences in the promoter regions of *rapL* and *ela3* revealed by MEME. **C** Site-directed mutagenesis of the conserved motifs in the signature sequence possibly recognized by RapH. The relative conserved 4-nt at both ends of the signature sequence are all mutated to GGGG, resulting in the mutated promoters, *rapLpmut* and *ela3pmut*. **D** Chromogenic assays of *S. coelicolor* M1146 containing the mutated promoter-driven *gusA* reporter and/or pIB-*rapH* on AS-1 agar plates. After mutagenesis of the signature RapH-binding sequence, chromogenic assays were conducted. Upon site-specific mutagenesis of the putative RapH-binding sequence in the promoter regions of *rapL* and *ela3*, the changes of blue color disappear, indicating RapH could not recognize the mutated binding site, thereby losing the ability to activate the expression of the *gusA* reporter gene

To better understand the regulation of RapH on the transcription of *rapL* and *ela3*, we identified the transcription start sites (TSSs) of these two genes using 5′-RACE. Total RNA was extracted from the fermentation culture of *S. rapamycinicus* collected after 5 days of growth. We showed that the TSSs of *rapL* and *ela3* were localized to two guanines (G) at 195-nt and 57-nt upstream of the start codons of these two genes, respectively. Then, the putative promoter -35 and -10 regions of these two genes, which were similar to the -35 and -10 regions of the reported *Streptomyces* promoters (Strohl. 1992), were proposed (Fig. 6). Based on the positions of the RapH-binding sites relative to the TSSs, binding of RapH to the promoter regions of *rapL* and *ela3* may enhance the recruitment of RNA polymerase, thereby activating their transcription.

Discussion

In this study, we showed that RapH, a cluster-situated regulator harbored in the rapamycin BGC, was involved in cross-regulation of the biosynthesis of rapamycin and elaiophylin co-produced by *S. rapamycinicus*. Through the GUS reporter system combined with transcriptional analysis, four target genes or operons, namely, *rapLMNO*/*rapH* in the rapamycin BGC and *ela3/ela9* in the elaiophylin BGC, were found to be possibly activated directly by RapH. Because the RapH-binding motif was close to the start codon of *rapK* (Fig. 6), we speculated that RapH binding could sterically block the access of RNA polymerase, thereby repressing the transcription of the operon *rapKJI* directly. However, we could not exclude the possibility of an indirect role in the regulation of *rapK* expression derived from RapH-mediated repression of some *rapK* activators.

Then, the possible molecular mechanism for RapH-mediated regulation of rapamycin and elaiophylin biosynthesis was proposed. The gene *rapL* encodes a lysine cyclodeaminase responsible for the formation of L-lysine-derived L-pipecolic acid, which is then inserted into the polyketide chain to form pre-rapamycin (Schwecke et al. 1995; Yoo et al. 2017). *rapI*, *rapJ*, *rapM*, *rapN*, and *rapO* are required for post-PKS modification at positions of C9, C16, C27, and C39 in rapamycin biosynthesis, including *O*-methylation and hydroxylation (Chung et al. 2001; Yoo et al. 2017). *rapK* encodes a chorismatase involved in the biosynthesis of DHCHC (the starter unit for rapamycin biosynthesis) (Andexer et al. 2011). Thus, RapH may enhance rapamycin biosynthesis possibly by increasing L-pipecolic acid supply and promoting the modifications at positions of C16 and C27 by activating *rapLMNO* transcription while also inhibiting the biosynthesis of DHCHC and the modifications at positions of C9 and C39 by repressing *rapKJI* expression. Therefore, RapH-mediated regulation of these target genes may enable the biosynthesis of the final product rapamycin or the pathway intermediates at a reasonable level, thereby avoiding its toxic effects on host cells. Two direct targets of

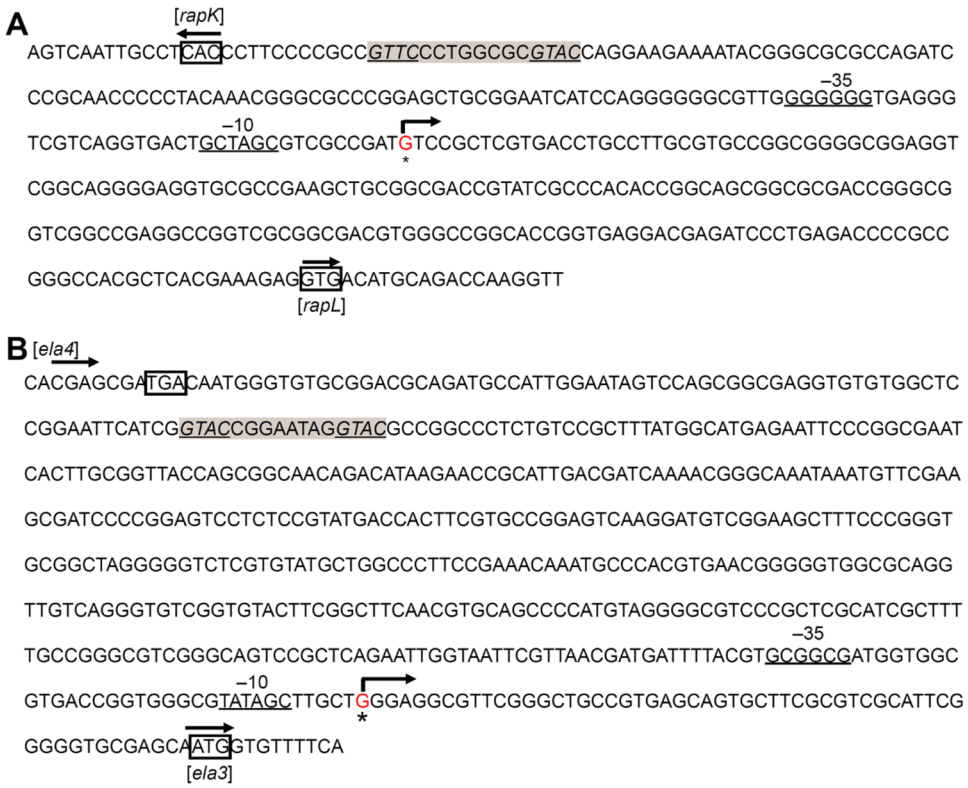

Fig. 6 Illustration of the RapH-binding sequence in the promoter regions of three target genes, *rapK*, *rapL* (**A**) and *ela3* (**B**). The transcription start site (TSS) is indicated by a bent arrow and an asterisk and the putative -10 and -35 elements of the promoters are underlined. The start or stop codons are indicated by black boxes. The RapH DNA-binding sequences are shaded and the relative conserved 4-nt palindrome sequences are underlined

RapH identified in the elaiophylin BGC are *ela3* and *ela9*, which encode a LuxR family regulator and a hypothetical protein, respectively. Accordingly, RapH may participate in the regulation of elaiophylin biosynthesis directly mediated by *ela3* and *ela9*. The role of RapH in the transcription of *elaMNOP*, *ela54*, and *ela6* could be exerted in a cascade-like manner mediated by the LuxR family regulator encoded by *ela3*. In addition, we also showed that RapH functioned as an auto-activator, suggesting that its role in the regulation of rapamycin and elaiophylin biosynthesis showed a positive feedback manner.

The observed RapH-mediated crossregulation of rapamycin and elaiophylin biosynthesis further highlighted the complexity of regulation of antibiotic biosynthesis in *S. rapamycinicus*. Although the biological significance of RapH-mediated regulation remains unknown, it may confer *S. rapamycinicus* with a competitive advantage against other biological species because these two antibiotics (rapamycin and elaiophylin) function synergistically to inhibit the growth of *Candida albicans* (Fang et al. 2000). Co-ordinated regulation of two disparate antibiotic BGCs by the cluster-situated regulators harbored within one BGC has also been reported for other cluster-situated regulators in the genus *Streptomyces* (McLean et al. 2019). For example, in *Streptomyces avermitilis*, the LAL family regulator AveR harbored in the avermectin BGC was shown to positively regulate avermectin biosynthesis while inhibiting oligomycin production (Guo et al. 2010). In *Streptomyces albus* S4, the biosynthesis of antimycin (an anticancer compound) was found to be directly regulated by the PAS-LuxR family cluster-situated regulator FscRI of the polyene antifungal compound candicidin (McLean et al. 2016). In addition, a TetR-family cluster-situated regulator from the geldanamycin BGC was shown to be involved in controlling geldanamycin and elaiophylin biosynthesis in *Streptomyces autolyticus* CGMCC051 (Jiang et al. 2017). The wide distribution of cluster-situated regulator-mediated crossregulation of disparate BGCs may signify a conserved strategy through which streptomycetes co-ordinately synthesize selected natural products, thereby conferring them a competitive advantage in the living environment.

LAL family regulators, which are characterized by an unusual large size harboring an ATP/GTP-binding domain at the N-terminus and a LuxR-like HTH DNA-binding domain at the C-terminus (Fig. S7) (Schrijver and Mot. 1999), are widely distributed and are mainly situated in gene clusters responsible for type I polyketide biosynthesis in the genus of *Streptomyces*. To date, more than 30 cluster-situated LAL family regulators have been functionally identified (Table S4). However, the regulatory mechanisms of only a few of these regulator have been elucidated, including NemR from the nemaketin BGC in *Streptomyces cyaneogriseus* (Li et al. 2019), AveR from the avermectin BGC in *S. avermitilis* (Guo et al. 2010), MilR from the milbemycin BGC in *S. milbemycinicus* (Zhang et al. 2016), SlnR from the salinomycin BGC in *Streptomyces albus* (Zhu et al. 2017), PimR from the pimaricin BGC in *Streptomyces natalensis* (Barreales et al. 2018), and StaR from the staurosporine BGC in *S. fradiae* CGMCC 4.576 (Guan et al. 2019). Besides AveR and RapH, which are involved in crossregulation of the biosynthesis of two antibiotics, all other LAL regulators were found to function as transcriptional activators of the gene cluster in which they are located. Further studies are needed to determine whether these LAL family regulators also regulate the biosynthesis of other antibiotics in the corresponding streptomycetes. In addition, the defined binding motifs of LAL family regulators identified to date are diverse, and this may reflect the diversity of the DNA-binding domains of these LAL family regulators in *Streptomyces* (Fig. S7).

RapH was previously identified as a pathway-specific regulator for rapamycin biosynthesis (Kuscer et al. 2007). Here, we showed that RapH actually functioned as a pleiotropic regulator. In future research, RNA-sequencing combined with chromatin immunoprecipitation sequencing (ChIP-seq) may be employed to determine whether RapH is also involved in the regulation of other physiological processes, such as the biosynthesis of other natural products. Such analysis will improve our understanding of the regulatory mechanisms of RapH in *S. rapamycinicus*.

Supplementary Information The online version contains supplementary material available at https://doi.org/10.1007/s00253-022-11847-9.

Author contribution YHL and JZT conceived and designed the study. WYH, JXM, JZT, and GSZ performed the experiments. WWF, YHL, and WHJ supervised the experiments. AAZ performed the bioinformatics analysis. WYH and YHL wrote the manuscript. All authors read and approved the final manuscript.

Funding This study was supported by the National Natural Science Foundation of China (31770088 and 31970083) and the National Key Research and Development Program (2019YFA0905400, 2021YFC2100600, and 2018YFA0903700).

Declarations

Conflicts of interest The authors declare no competing interests..

References

Andexer JN, Kendrew SG, Nur-e-Alam M, Lazos O, Foster TA, Zimmermann AS, Warneck TD, Suthar D, Coates NJ, Koehn FE, Skotnicki JS, Carter GT, Gregory MA, Martin CJ, Moss SJ, Leadlay PF, Wilkinson B (2011) Biosynthesis of the immunosuppressants FK506, FK520, and rapamycin involves a previously undescribed family of enzymes acting on chorismate. Proc Natl Acad Sci U S A 108:4776–4781

Aparicio JF, Molnar I, Schwecke T, Konig A, Haydock SF, Khaw LE, Staunton J, Leadlay PF (1996) Organization of the biosynthetic gene cluster for rapamycin in *Streptomyces hygroscopicus*: analysis of the enzymatic domains in the modular polyketide synthase. Gene 169:9–16

Argyriou P, Economopoulou P, Papageorgiou S (2012) The Role of mTOR inhibitors for the treatment of B-Cell lymphomas. Adv Hematol 2012:435342

Barreales EG, Vicente CM, de Pedro A, Santos-Aberturas J, Aparicio JF (2018) Promoter engineering reveals the importance of heptameric direct repeats for DNA binding by streptomyces antibiotic regulatory protein-large ATP-binding regulator of the LuxR family (SARP-LAL) regulators in *Streptomyces natalensis*. Appl Environ Microbiol 84:e00246

Chung L, Liu L, Patel S, Carney JR, Reeves CD (2001) Deletion of *rapQONML* from the rapamycin gene cluster of *Streptomyces hygroscopicus* gives production of the 16-O-desmethyl-27-desmethoxy analog. J Antibiot (tokyo) 54:250–256

Fang A, Wong GK, Demain AL (2000) Enhancement of the antifungal activity of rapamycin by the coproduced elaiophylin and nigericin. J Antibiot (tokyo) 53:158–162

Gomez-Escribano JP, Bibb MJ (2011) Engineering *Streptomyces coelicolor* for heterologous expression of secondary metabolite gene clusters. Microb Biotechnol 4:207–215

Gregory MA, Gaisser S, Lill RE, Hong H, Sheridan RM, Wilkinson B, Petkovic H, Weston AJ, Carletti I, Lee HL, Staunton J, Leadlay PF (2004) Isolation and characterization of pre-rapamycin, the first macrocyclic intermediate in the biosynthesis of the immunosuppressant rapamycin by *S. hygroscopicus*. Angew Chem Int Ed Engl 43:2551–2553

Guan H, Li Y, Zheng J, Liu N, Zhang J, Tan H (2019) Important role of a LAL regulator StaR in the staurosporine biosynthesis and high-production of *Streptomyces fradiae* CGMCC 4.576. Sci China Life Sci 62:1638–1654

Gui M, Zhang MX, Wu WH, Sun P (2019) Natural occurrence, bioactivity and biosynthesis of elaiophylin analogues. Molecules 24:3840

Guo J, Zhao JL, Li LL, Chen Z, Wen Y, Li JL (2010) The pathway-specific regulator AveR from *Streptomyces avermitilis* positively regulates avermectin production while it negatively affects oligomycin biosynthesis. Mol Genet Genomics 283:123–133

Hamedi J, Mohammadipanah F, Klenk HP, Potter G, Schumann P, Sproer C, von Jan M, Kroppenstedt RM (2010) *Streptomyces iranensis* sp. nov., isolated from soil. Int J Syst Evol Microbiol 60:1504–1509

Hammann P, Kretzschmar G, Seibert G (1990) Secondary metabolites by chemical screening. 7. I. Elaiophylin derivatives and their biological activities. J Antibiot (tokyo) 43:1431–1440

Haydock SF, Mironenko T, Ghoorahoo HI, Leadlay PF (2004) The putative elaiophylin biosynthetic gene cluster in *Streptomyces* sp. DSM4137 is adjacent to genes encoding adenosylcobalamin-dependent methylmalonyl CoA mutase and to genes for synthesis of cobalamin. J Biotechnol 113:55–68

Horn F, Schroeckh V, Netzker T, Guthke R, Brakhage AA, Linde J (2014) Draft genome sequence of *Streptomyces iranensis*. Genome Announc 2:e00616

Houchens DP, Ovejera AA, Riblet SM, Slagel DE (1983) Human brain tumor xenografts in nude mice as a chemotherapy model. Eur J Cancer Clin Oncol 19:799–805

Huang H, Ren SX, Yang S, Hu HF (2015a) Comparative analysis of rapamycin biosynthesis clusters between *Actinoplanes* sp. N902–109 and *Streptomyces hygroscopicus* ATCC29253. Chin J Nat Med 13:90–98

Huang H, Zheng GS, Jiang WH, Hu HF, Lu YH (2015b) One-step high-efficiency CRISPR/Cas9-mediated genome editing in *Streptomyces*. Acta Bioch Bioph Sin 47:231–243

Jiang M, Yin M, Wu S, Han X, Ji K, Wen M, Lu T (2017) GdmRIII, a TetR Family Transcriptional Regulator, Controls Geldanamycin and Elaiophylin Biosynthesis in *Streptomyces autolyticus* CGMCC0516. Sci Rep 7:4803

Kieser T, Bibb MJ, Buttner MJ, Chater KF (2000) Practical Streptomyces genetics. John Innes Foundation, Norwich, England

Klassen JL, Lee SR, Poulsen M, Beemelmanns C, Kim KH (2019) Efomycins K and L from a termite-associated *Streptomyces* sp. M56 and their putative biosynthetic origin. Front Microbiol 10:1739

Konig A, Schwecke T, Molnar I, Bohm GA, Lowden PA, Staunton J, Leadlay PF (1997) The pipecolate-incorporating enzyme for the biosynthesis of the immunosuppressant rapamycin-nucleotide sequence analysis, disruption and heterologous expression of *rapP* from *Streptomyces hygroscopicus*. Eur J Biochem 247:526–534

Kuscer E, Coates N, Challis I, Gregory M, Wilkinson B, Sheridan R, Petkovic H (2007) Roles of *rapH* and *rapG* in positive regulation of rapamycin biosynthesis in *Streptomyces hygroscopicus*. J Bacteriol 189:4756–4763

Li C, He H, Wang J, Liu H, Wang H, Zhu Y, Wang X, Zhang Y, Xiang W (2019) Characterization of a LAL-type regulator NemR in nemadectin biosynthesis and its application for increasing nemadectin production in *Streptomyces cyaneogriseus*. Sci China Life Sci 62:394–405

Liu H, Naismith JH (2008) An efficient one-step site-directed deletion, insertion, single and multiple-site plasmid mutagenesis protocol. BMC Biotechnol 8:91

Livak KJ, Schmittgen TD (2001) Analysis of relative gene expression data using real-time quantitative PCR and the 2(-Delta Delta C(T)) Method. Methods 25:402–408

Malagelada C, Jin ZH, Jackson-Lewis V, Przedborski S, Greene LA (2010) Rapamycin protects against neuron death in *in vitro* and *in vivo* models of Parkinson's disease. J Neurosci 30:1166–1175

Martel RR, Klicius J, Galet S (1977) Inhibition of the immune response by rapamycin, a new antifungal antibiotic. Can J Physiol Pharmacol 55:48–51

McLean TC, Hoskisson PA, Seipke RF (2016) Coordinate regulation of antimycin and candicidin biosynthesis. mSphere 1:e00305

McLean TC, Wilkinson B, Hutchings MI, Devine R (2019) Dissolution of the disparate: co-ordinate regulation in antibiotic biosynthesis. Antibiotics (basel) 8:83

Myronovskyi M, Welle E, Fedorenko V, Luzhetskyy A (2011) Beta-glucuronidase as a sensitive and versatile reporter in *Actinomycetes*. Appl Environ Microbiol 77:5370–5383

Paiva NL, Demain AL, Roberts MF (1991) Incorporation of acetate, propionate, and methionine into rapamycin by *Streptomyces hygroscopicus*. J Nat Prod 54:167–177

Pan T, Kondo S, Zhu W, Xie W, Jankovic J, Le W (2008) Neuroprotection of rapamycin in lactacystin-induced neurodegeneration via autophagy enhancement. Neurobiol Dis 32:16–25

Park SR, Yoo YJ, Ban YH, Yoon YJ (2010) Biosynthesis of rapamycin and its regulation: past achievements and recent progress. J Antibiot (tokyo) 63:434–441

Schrijver A, Mot R (1999) A subfamily of MalT-related ATP-dependent regulators in the LuxR family. Microbiology (reading) 145(Pt 6):1287–1288

Schwecke T, Aparicio JF, Molnar I, Konig A, Khaw LE, Haydock SF, Oliynyk M, Caffrey P, Cortes J, Lester JB (1995) The biosynthetic gene cluster for the polyketide immunosuppressant rapamycin. Proc Natl Acad Sci U S A 92:7839–7843

Strohl WR (1992) Compilation and analysis of DNA sequences associated with apparent *streptomycete* promoters. Nucleic Acids Res 20:961–974

Tain LS, Mortiboys H, Tao RN, Ziviani E, Bandmann O, Whitworth AJ (2009) Rapamycin activation of 4E-BP prevents parkinsonian dopaminergic neuron loss. Nat Neurosci 12:1129–1135

Vezina C, Kudelski A, Sehgal SN (1975) Rapamycin (AY-22,989), a new antifungal antibiotic. I. Taxonomy of the producing streptomycete and isolation of the active principle. J Antibiot (tokyo) 28:721–726

Wilkinson CJ, Hughes-Thomas ZA, Martin CJ, Bohm I, Mironenko T, Deacon M, Wheatcroft M, Wirtz G, Staunton J, Leadlay PF (2002) Increasing the efficiency of heterologous promoters in *actinomycetes*. J Mol Microbiol 4:417–426

Wu C, Tan Y, Gan M, Wang Y, Guan Y, Hu X, Zhou H, Shang X, You X, Yang Z, Xiao C (2013) Identification of elaiophylin derivatives from the marine-derived actinomycete *Streptomyces* sp. 7–145 using PCR-based screening. J Nat Prod 76:2153–2157

Yoo YJ, Hwang JY, Shin H, Cui H, Lee J, Yoon YJ (2015) Characterization of negative regulatory genes for the biosynthesis of rapamycin in *Streptomyces rapamycinicus* and its application for improved production. J Ind Microbiol Biotechnol 42:125–135

Yoo YJ, Kim H, Park SR, Yoon YJ (2017) An overview of rapamycin: from discovery to future perspectives. J Ind Microbiol Biotechnol 44:537–553

Zhang YY, He HR, Liu H, Wang HY, Wang XJ, Xiang WS (2016) Characterization of a pathway-specific activator of milbemycin biosynthesis and improved milbemycin production by its overexpression in *Streptomyces bingchenggensis*. Microb Cell Fact 15:152

Zhao X, Fang Y, Yang Y, Qin Y, Wu P, Wang T, Lai H, Meng L, Wang D, Zheng Z, Lu X, Zhang H, Gao Q, Zhou J, Ma D (2015) Elaiophylin, a novel autophagy inhibitor, exerts antitumor activity as a single agent in ovarian cancer cells. Autophagy 11:1849–1863

Zhou HY, Huang SL (2012) Current development of the second generation of mTOR inhibitors as anticancer agents. Chin J Cancer 31:8–18

Zhu Z, Li H, Yu P, Guo Y, Luo S, Chen Z, Mao X, Guan W, Li Y (2017) SlnR is a positive pathway-specific regulator for salinomycin biosynthesis in *Streptomyces albus*. Appl Microbiol Biotechnol 101:1547–1557